Heliyon 5 (2019) e02155

Contents lists available at ScienceDirect

Heliyon

journal homepage: www.heliyon.com

DFT investigation of role of N – H···O and N – H···π interactions in the stabilization of the hydrogen bonded complexes of anisole with aromatic amines

Anil Singh Rajpurohit [a], R. Rajesh [b], R. Raj Muhamed [c], M. Jaccob [a], A. Justin Adaikala Baskar [a], V. Kannappan [d,*]

[a] Department of Chemistry, Loyola College, Chennai 600 034, India
[b] Department of Physics, Sri Vijay Vidyalaya College of Arts and Science, Nallampalli, Dharmapuri, 636807, India
[c] Department of Physics, Jamal Mohamed College, Tiruchirappalli, 621 004, India
[d] Department of Chemistry, Presidency College, Chennai, 600 005, India

ARTICLE INFO

Keywords:
Theoretical chemistry
DFT study
Anisole amine complexes

ABSTRACT

Theoretical investigations have been performed on hydrogen (H-) bonded complexes of two aromatic amines with anisole to investigate the effect of the methyl substituent on N– H···O and N—H···π interactions. Natural bond orbital (NBO) and quantum theory of atoms in molecules (QTAIM) analyses were done to elucidate the nature of H- bonding. In 1:1 complexes, the total interaction energy of N-methylaniline complex is higher than that of aniline complex. The existence of bond critical point between N–H of amine and oxygen of anisole confirms weak hydrogen bonding. The energy decomposition analysis showed the role of CT in stabilizing complexes.

1. Introduction

Aliphatic and aromatic ethers act as proton acceptors and they are used as solvents in many chemical industries. Aromatic amines such as aniline can be considered as models for biochemical systems such as nucleobases in DNA and RNA. The hydrogen bonding between base pairs in nucleic acid holds them together [1, 2, 3]. In proteins, the amino group interaction with π-electron cloud of aromatic ring was detected [4, 5]. Due to common existence of amino functional group in organic molecules, various studies have been carried out to characterize its interaction ability, effects on geometry and other physical properties. Amine-based solid adsorbents are used to capture flue gases such as CO_2, SO_2 by sorption [6]. Parthipan and Thenappan studied the dielectric and thermodynamic behavior of binary mixtures of anisole and aniline at different composition and temperatures to understand the molecular structures and intermolecular interactions [7]. Piani *et al* concluded from the study of anisole-ammonia complex that the red shift of $S_1 \leftarrow S_0$ transition in the Resonance-enhanced multi photon ionization spectrum is due to the interaction of hydrogen atom and lone pair on the nitrogen atom of the ammonia with π-electron density of aromatic ring and hydrogen atom of the methoxy group of the anisole respectively [8]. Recently, we established the formation of hydrogen bonded complexes between anisole and aromatic amines through ultrasonic and UV spectral studies (experimental). We found from the thermodynamic data of these complexes that of the two complexes, aniline formed more stable complex with anisole than N-methylaniline [9].

Major work on hydrogen-bonded complexes between aromatic amines which serve as proton donors is directed toward the frequency shifts infrared, ultraviolet and NMR spectra of amines as a result of complex formation [10]. Although there are thermodynamic data for the self-association of aniline and association of aniline and N-methylaniline with some heterocyclic compounds, there is no theoretical investigation of such studies with aromatic ethers [11]. Investigation of association of aniline or *N*-methylaniline with aromatic compounds indicated that they form 1:1 complexes in cyclohexane and also there was self-association of protic amine. These studies also revealed that formation of the N–H···π hydrogen bond of the electron-rich aromatic group may compete with N–H···N hydrogen bond [12]. The N–H···*π* hydrogen bonding interaction was studied for the 1-naphthylamine system and several proton donors by UV spectral method [13]. In this paper we present the results obtained in the DFT analysis of hydrogen bonded complexes of anisole with two aromatic amines (aniline and N-methylaniline), especially the role of N–H···O and N– H···π interactions in stabilizing these complexes.

* Corresponding author.
E-mail address: venu_kannappan@rediffmail.com (V. Kannappan).

https://doi.org/10.1016/j.heliyon.2019.e02155
Received 16 May 2019; Received in revised form 17 July 2019; Accepted 22 July 2019

2. Theory/calculation

Quantum chemical calculations of the complexes of anisole and two aromatic amines were performed by using Gaussian 09 program package [14]. The geometry optimizations of the isolated monomers and the hydrogen-bonded complexes were performed using ωB97X-D3 hybrid functional [15] which includes both long range exchange and Grimme's dispersion of D3 version [16]. The 6–311++G (d,p) basis set was used for all atoms of the complexes [17, 18]. It may be pointed out that no imaginary vibrational frequencies were shown by the optimized geometries of stable complexes. In the calculation of interaction energies, counterpoise method was used to calculate the Basis set superposition error (BSSE) [19]. A conductor-like polarizable continuum model (CPCM) as implemented in GAUSSIAN 09 was applied to compute the electronic spectra of different hydrogen bonded complexes in n-hexane solvent [20, 21]. Arguslab 4.0.1 molecular modeling program was used to generate molecular electrostatic potential map [22]. Natural bond orbital (NBO) analysis was done to study the energy gap and hybridization bonds, natural atomic charge and electron transfer between levels in the hydrogen bonded complexes [23, 24]. AIM2000 was used to carry out topological analysis of the electron density of hydrogen bonded complexes and the corresponding wave function has been generated at ωB97X-D/6–311++G (d,p)level [25]. Chemcraft graphical program was used for visualization purposes [26].

3. Results and discussion

3.1. Optimized geometries and interaction energies

The hydrogen atoms of amino group of aniline and N-methylaniline can interact with oxygen atom or π-electron cloud of aromatic ring of anisole forming 1:1 and/or 1:2 complexes [27, 28, 29]. The structures of the 1:1 complexes (**a1** and **n1)** were built by placing the amino group hydrogen of aniline and N-methylaniline close to the ethereal oxygen atom of anisole. However, in the 1:1 complexes (**a2** and **n2)** stacking structure is observed in which the monomers are arranged in stacked fashion such that their substituents lie above the aromatic rings of one another (Fig. 1). In the case of1:2 complexes (**a3)**, one aniline and two anisole molecules are used for the N—H···O type hydrogen bonding. Absence of imaginary frequencies in all these structures confirms true minima. The structure of aniline (**a**) differs from N-methylaniline (**n**) just by methyl group substitution on the nitrogen atom. The H–N–H angle of aniline is 3.1° smaller than the H–N–CH_3 angle of N-methylaniline. With introduction of methyl group on nitrogen atom, the molecule becomes more planar with decrease in C–N and N–H bond length [30].

Table 1 contains the counterpoise corrected interaction energies between aromatic amines and anisole along with structural parameters of optimized geometry of monomers and complexes. The interaction

Table 1
Structural parameters such as bond lengths (Å), bond angles (degrees) and interaction energies (kJ/mol) of aniline, N-methylaniline and their hydrogen bonded complexes computed at the ωB97XD/6–311++G (d,p) level.

Complex	ΔE	N–H bond length	C–N bond length	N – H···X Interaction (X = O, C)		H – N – X angle (X = H, C_{Me})
				Distance	Angle	
A	-	1.008, 1.008	1.395	-	-	112.1
N	-	1.006	1.387	-	-	115.2
a1	-25.00	1.012,1.007	1.392	2.086	161.6	113.5
n1	-30.76	1.010	1.388	2.305	134.7	113.8
a2	-36.10	1.009,1.010	1.392	2.843, 2.856	126.5, 124.6	109.8
n2	-38.76	1.009	1.385	2.833	157.8	114.3
a3	-48.52	1.011,1.011	1.388	2.071, 2.071	163.3, 163.3	114.9

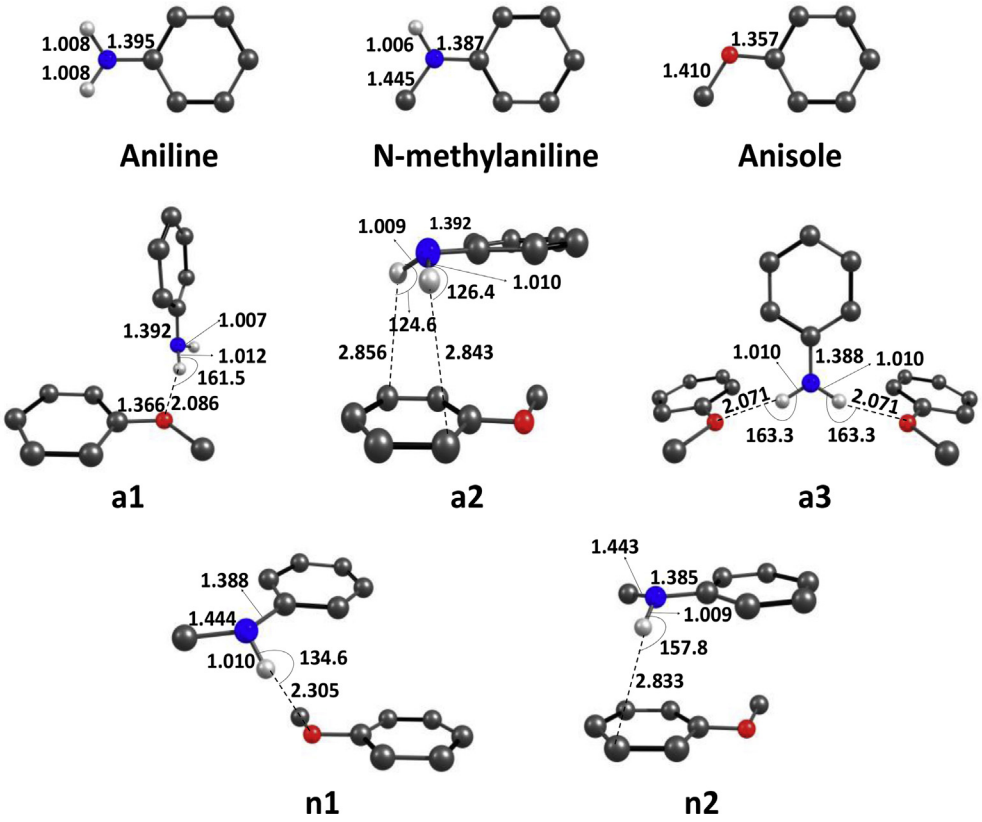

Fig. 1. Optimized geometries of aniline, N-methylaniline and their hydrogen bonded complexes calculated at the ωB97XD/6–311++G (d,p) level of the theory.

energies of stacking model of **a2** and **n2** depicting N–H···π type hydrogen bonding are -36.10 and -38.76 kJ/mol respectively. In 1:1 **a1** and **n1** complexes, the N–H···O interaction energies are -25 and -30.76 kJ/mol respectively. The calculated hydrogen bond lengths between H of amino group and O of anisole is 2.086 and 2.305 Å for the **a1** and.

n1 complexes, which is much less than N–H···π bond length in **a2** and **n2**. This difference is reflected in the N–H bond length. The **a1** and **n1** complexes have higher N–H bond elongation than in **a2** and **n2** complexes. This clearly shows that the interaction energy of **a2** and **n2** complexes includes other possible non-covalent interactions besides classical N–H···O hydrogen bonding. In **a1** and **n1,** the interaction energy includes only N–H···O interaction. The difference in interaction energy, N–H and N–H···O bond length between **a1** and **n1** is mainly due to effect of methyl group substitution. The interaction energy of **n1** is 5.76 kJ/mol lower than that of a1 complex. The **a3** complex has the interaction energy of-48.52 kJ/mol, which is the highest among all the possible complexes with shortest N–H···O distance of about 2.071Å. It may be noted that the formation of 1:2 complex (**a3**) formation is more probable only when aniline concentration is at least twice that of anisole concentration. In systems containing equi-molar concentration of amine and anisole the formation of 1:1 complex is more probable.

3.2. Surface electrostatic potential analysis

Whenever a covalent bond is formed between atoms with different electronegativity values, it polarizes electronic charge on atom towards the bond region. This leads to the potential difference across the molecular surface due to anisotropy of electronic density. Therefore electrostatic potential mapping can be used to determine the specific sites where intermolecular hydrogen bonding can take place. As shown in Fig. 2, the electrostatic component is more negative at oxygen atom than at aromatic ring in anisole molecule. In aniline and N-methylaniline, the hydrogen atom attached to nitrogen has higher positive electrostatic potential which shows that it can form H-bonding with anisole. Based on atom to atom interaction, the N—H···O type interaction seems to be stronger than N—H···π type interaction. But multiple intermolecular atoms interactions in stacking model of **a2** and **n2** complexes can compete with N–H···O interaction of **a1**, **n1** and **a3** complexes.

3.3. Vibrational analysis

The hydrogen bond existence can be characterized by N–H stretching vibration frequency and intensity. Fig. 3 shows the infrared spectra over the range 3500–3800 cm^{-1} for monomers and their anisole complexes. The results are summarized in Table 2. The symmetric and asymmetric primary amine peaks appear at 3611 and 3712 cm^{-1} respectively. For **a1** complex, both stretching vibrations of NH_2 group shift towards lower frequency at 3576 and 3699 cm^{-1}. In **a2** complex, the peaks appeared at 3600 and 3687 cm^{-1}. On comparison with **a1** complex, the NH_2 group stretching vibration of **a3** displays much higher downshifts at 3557 and 3656 cm^{-1}. The vibration band of N–H in N-methylaniline appeared at 3668 $cm^{-1}$for monomer and lower frequencies at 3630 and 3637 $cm^{-1}$for **n1** and **n2** complexes respectively. The results are consistent with experimental data [31].

Both in aniline and N-methylaniline the N–H···O type hydrogen bond complexes show higher red shifts of amino group frequency than in N–

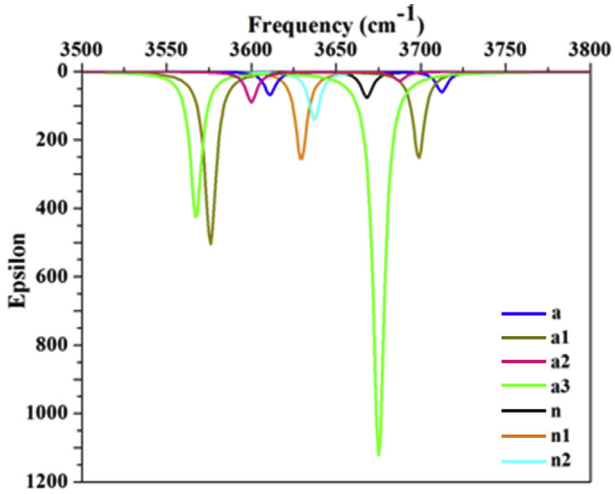

Fig. 3. Infrared spectra in the 3500-3800 cm^{-1} spectral range of isolated monomers (a and n) and their hydrogen bonded complexes (a1, a2, a3, n1, n2) computed with the ωB97XD/6–311++G (d,p) method.

Table 2
Calculated harmonic stretching vibrational frequencies (cm^{-1}) of N–H bond, epsilon and force constant (mDyneÅ^{-1}) of aniline, N-methylaniline and their hydrogen bonded complexes.

Complex	N–H frequency	Epsilon	Force constant
a	3611, 3712	68, 60	8.05, 8.92
n	3668	77	8.53
a1	3576, 3699	505, 252	7.92, 8.84
n1	3630	255	8.35
a2	3600, 3687	89, 27	8.01, 8.78
n2	3637	141	8.39
a3	3567, 3675	425, 1122	7.85, 8.77

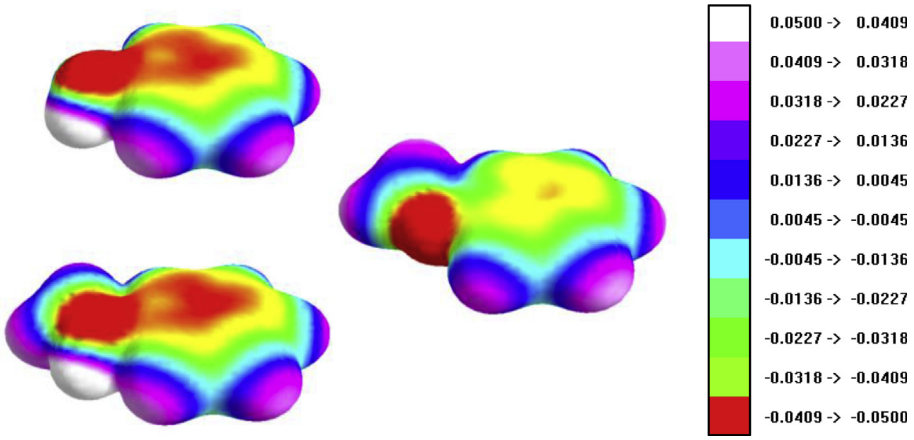

Fig. 2. Molecular electrostatic potential map (-0.05 to +0.05 Hartrees) on 0.007 a. u. isosurface of aniline, N-methylaniline and anisole molecules calculated using Austin Model 1 (AM1) parameterization.

H···π type hydrogen bond complexes. The extent of red shifts shows that the former type hydrogen bond is stronger than latter type. The increase in the strength of hydrogen bond lengthens the N– H bond by reducing force constant and varying infrared intensity [32].

3.4. Electronic spectra

The time dependent density functional theory is used to generate an overlay electronic spectra of monomers and all complexes in n-hexane solvent are shown in Fig. 4 and their electronic excitation energies and corresponding oscillator strengths are presented in Table 3. The calculated absorption bands in aniline were found at 222 nm and 253nm and in N-methylaniline at 228 nm and 260 nm were assigned to π→π* and n→π* transitions respectively. In aniline the π→π* transition mainly composed of a HOMO to LUMO+4 transition (62.72%). In the case of N-methylaniline, 64.98% of contribution observed from HOMO to LUMO+6 transition. Similarly major contributions for π→π* transition in all hydrogen bonded complexes are listed in Table 3. All the hydrogen bonded complexes show 3–9 nm red shift of π→π*transitions with respect to the transitions observed in their monomers. If we compare 1:1 complexes of aniline and N-methylaniline, the electronic spectra showed π→π* transition of stacking model complex absorbed at higher wavelength than complex with N– H···O ineraction. It may be noted that aniline based 1:2 N– H···O type complex showed the highest red shift. This red shift of transition displays existence of H- bonding between aromatic amines and anisole. Similar type of shifts was reported in the

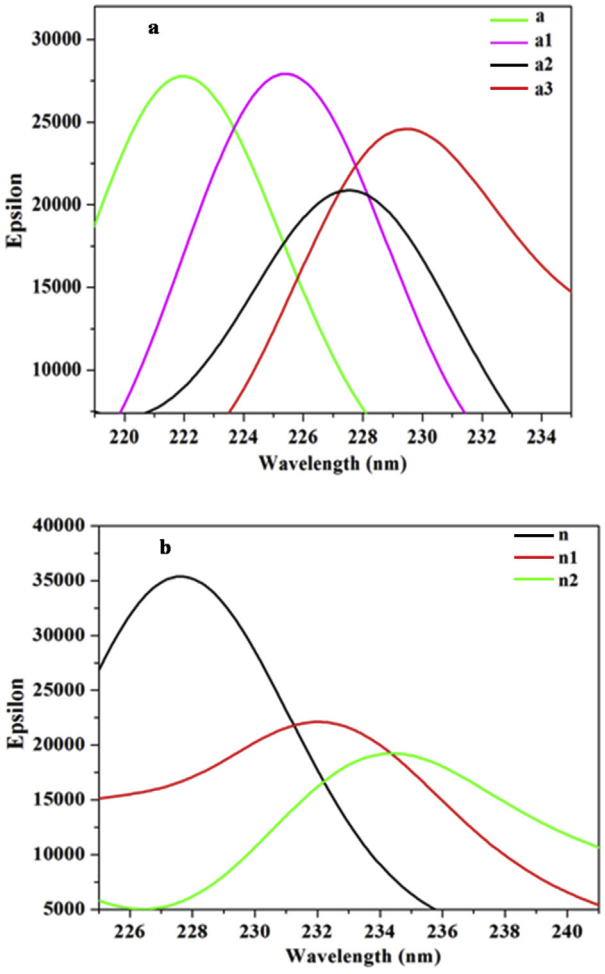

Fig. 4. Electronic absorption spectra for π→ π* transition of (a) a, a1, a2, a3 and (b) n, n1, n2 in n-hexane solvent calculated at the ωB97XD/6–311++G (d,p) level.

Table 3
Calculated wavelength (nm), corresponding epsilon, electronic excitation energies (eV), and orbitals involve in π→ π* transition along with major contribution (%) for monomers and their hydrogen bonded complexes.

complex	λ_{calc}	Epsilon	Excitation energy	Major contribution	% contribution
A	222	27774	5.59	HOMO→LUMO+4	62.72
N	228	35378	5.44	HOMO→LUMO+6	64.98
a1	225	27922	5.50	HOMO→LUMO+9	35.28
				HOMO→LUMO+10	27.38
n1	232	22118	5.34	HOMO→LUMO+10	32.00
a2	228	20872	5.44	HOMO→LUMO+1	25.92
n2	234	19237	5.30	HOMO→LUMO+10	21.78
a3	227	23864	5.46	HOMO→LUMO+17	25.92
	231	25721	5.37	HOMO→LUMO	27.38

experimental study of same model complexes through ultrasonic application [9]. It was concluded from results that methylation of aniline and hydrogen bonding are responsible to shift π→π* transition towards higher wavelength.

3.5. NBO analysis

3.5.1. Monomers

The hybridization state of a nitrogen atom and its effect on bonding order can provide clear image of methyl group effect on hydrogen bonding. Hybridization details with bond order and Wiberg total bond index of **a** and **n** based on the natural bond orbital (NBO) analysis is shown in Table 4. The nitrogen atom of aniline formed bonds with different atoms using different hybridized orbitals. In N-methylaniline, the presence of methyl substituent such pushes electron density towards nitrogen atom through inductive mechanism (+I effect). To stabilize these electrons, the s-character of methyl bonded hybrid orbital of nitrogen atom increases with decrease in p-character. This difference in methyl bonded hybrid orbital reduces s-character of remaining hybridized orbitals with increases in p-character. The decrease in s-character of hybridized orbital holding lone pair reduces electron stabilization and increase in p-character make possible for lone pair electron to interact with π-electron of aromatic ring more firmly. This is reflected by decrease in mulliken charge on nitrogen atom from -0.348 in aniline to -0.136 in N-methylaniline. The combine effect of lone pair electron delocalization into aromatic ring and decrease in s-character of hybrid orbital of nitrogen in C–N bond increases C–N bond order and Wiberg total bond index (number of covalent bonds) on nitrogen atom. Therefore N-methylaniline becomes more planar than aniline.

The decrease in s-character of hybrid orbital of nitrogen in N–H bond makes electron free from nitrogen electronegative pull. As shown in Table 5, It was also observed that electron delocalization took place from $\sigma_{N\text{-}H}\rightarrow\sigma^*_{C\text{–}C(amine)}$through hyper conjugation. The shared pair of electrons of N–H bond in N-methylaniline is more readily available for delocalization than in aniline. Hence bond order of N–H bond decreases. The better hyper conjugation in N-methylaniline increases polarity and reduces N–H bond length. These results show dominance of hyper conjugation effect over increase in p-character in N–H bond of N-methylaniline. The overall effect increases ionic character ($i_{N\text{-}H}$) of N–H bond in N-methylaniline than in aniline.

3.5.2. Hydrogen bonded complexes

The natural bonding orbital analysis has been reliable tool to study the charge transfer from donor to acceptor. In this method the electronic wave function is interpreted in terms of a set of occupied Lewis and a set of unoccupied non-Lewis localized orbitals. The second order perturbation energy $E^{(2)}$ associated with hydrogen bonding between a donor (i) and acceptor (j) is given by Eq. (1)

Table 4
Change in %s and %p character of hybridized orbitals, bond parameters and natural ionicity parameter of monomers.

Monomer	Hybridization of natural hybrid orbitals of nitrogen and its bonded atoms				Wiberg total bond index of N atom	Bond order		$i_{N\text{-}H}$*
	$C_{(Me)}$–N	$C_{(Ar)}$-N	N–H	N lone pair		C–N	N–H	
a	-	$s^{28.0\%}p^{72.0\%}$ $s^{37.8\%}p^{62.2\%}$	$s^{25.8\%}p^{74.2\%}$ $s^{100\%}$	$s^{10.5\%}p^{89.5\%}$	2.95	0.933	0.922	0.377
n	$s^{25.4\%}p^{74.6\%}s^{32.9\%}p^{67.1\%}$	$s^{28.2\%}p^{71.8\%}$ $s^{37.0\%}p^{63.0\%}$	$s^{24.5\%}p^{75.5\%}$ $s^{100\%}$	$s^{5.6\%}p^{94.4\%}$	3.13	1.035	0.917	0.381

*For a pure covalent bond $i_{N\text{-}H}$ is zero. As the value reaches closer to -1 or +1, the ionic character of bond increases.

Table 5
NBO Values of occupancy of donor and acceptor (in a.u.) and $E^{(2)}$ (kJ/mol) of monomers.

Monomer	Donor (occupancy)	Acceptor (occupancy)	$\Delta E^{(2)}$
A	$\sigma_{N\text{-}H}$ (1.988)	$\sigma^*_{C-C(amine)}$ (0.024)	18.28
	$\sigma_{N\text{-}H}$ (1.988)	$\sigma^*_{C-C(amine)}$ (0.024)	18.33
N	$\sigma_{N\text{-}H}$ (1.983)	$\sigma^*_{C-C(amine)}$ (0.025)	19.33

$$E_{ij}^{(2)} = q_i \frac{|F_{ij}|^2}{\varepsilon_j - \varepsilon_i} \quad (1)$$

Where q_i is the occupancy of i^{th} donor orbital, ε_i and ε_j are the respective donor and acceptor orbital energies and $F_{i,j}$ is the off-diagonal NBO Fock matrix element [33]. The NBOs involve in charge transfer between donor and acceptor are shown in Fig. 5. The transfer of electron density from the oxygen lone pair electron (n_{LPO})or π-electron cloud on aromatic ring of the anisole (donor) to the σ^*_{N-H} orbital of the acceptor, stabilizes the formed complexes. In stacking model, the charge transfer from π-electron cloud on aromatic ring of the aromatic amine to σ^*_{C-H} orbital of methoxy group of anisole was also considered. The second-order orbital interaction energies $E^{(2)}$, occupancies of acceptor and donor, amount of charge transferred and NBO deletion energy of hydrogen bonded complexes are listed in Table 6. In all complexes, there is small amount of charge transfer in the range of 0.16–0.36 a. u. from donor to acceptor. Both lone pair of oxygen atom of anisole are involved in charge transfer process. The stabilizing energy for $n_{LPO} \rightarrow \sigma^*_{N-H}$ orbitals charge transfer in **a1**, **n1** and **a3** are 20.81, 8.45 and 43.04 kJ/mol respectively. In stacking model, the stabilizing energy due to charge transfer from $\pi_{C=C(amine)} \rightarrow \sigma^*_{C-H}$ and $\pi_{C=C(anisole)} \rightarrow \sigma^*_{N-H}$is1.76 and 3.22 kJ/mol in **a2** and 1.42 and 2.42 kJ/mol**n2**complexes respectively. This results shows that charge transfer in N- H···π type hydrogen bond complexes is weaker than in N- H···O type complexes. The **a3** complex shows highest stabilization energy than any other complex through $n_{LPO} \rightarrow \sigma^*_{N-H}$ charge transfer. The stability of hydrogen bonded complexes is reduced upon deleting the respective charge transfer orbitals involved in the H-bonding interactions. This specifies that higher NBO deletion energies is often associated with strong H-bonded complexes. Higher NBO deletion energy indicates higher destabilization of complexes. From NBO analysis it is found that both N- H···O and N- H···π type interactions of 1:1 N-methylaniline-anisole complex involves lesser charge transfer than in aniline complexes. Therefore, total interaction energy of N-methylaniline complexes is higher than aniline complex is due to higher ionic character (electrostatic interaction) of N–H bond. But it was reported experimentally that aniline can form more stable complex than N-methylaniline with anisole [9]. This may be due to the ability of aniline to form 1:2 complex along with 1:1 complexes, which is more stable than 1:1 complexes of N-methylaniline.

3.6. Topography of electron density of the hydrogen bonded complexes

The presence of the hydrogen bonding is confirmed by topological analysis of the electron density using Bader's quantum theory Atoms in molecules (QTAIM). This method calculates the electron density ρ(r) and the Laplacian$\nabla^2\rho(r)$ of the electron density ρ(r)along bond path. The presence of a (3,-1) bond critical point (BCP) between hydrogen donor and acceptor is considered as indicator of hydrogen bonding. The values of the electron density ρ(r) and the Laplacian of the electron density $\nabla^2\rho(r)$at the BCP measure the strength of hydrogen bonding. The negative $\nabla^2\rho(r)$ value indicate electron accumulation and positive value indicate electron depletion. Koch and Popelier proposed the criteria for the existence of hydrogen bonding between atoms [34, 35]. For hydrogen bonding, ρ(r) is in the range of 0.002–0.034 a. u. and $\nabla^2\rho(r)$ lies within 0.024–0.139 a. u. The relation between topological parameters and $\nabla^2\rho(r)$at the BCP can be obtained from virial theorem using Eqs. (2) and (3)

$$\left(\frac{1}{4}\right)\nabla^2\rho(r) = 2G(r) + V(r) \quad (2)$$

$$H(r) = G(r) + V(r) \quad (3)$$

Where G(r), V(r) and H(r) are the electron kinetic energy density, electron potential energy density and total electron energy density at BCP. It has been found $\nabla^2\rho(r) > 0$ and $H(r) > 0$ for weak and medium strength H- bonding and $\nabla^2\rho(r) > 0$ and $H(r) < 0$ for strong H- bonding. Further, if $\nabla^2\rho(r) < 0$ and $H(r) < 0$ then there is only covalent bonding.

As shown in Fig. 6, both N- H···O and N- H···π type of intermolecular hydrogen bonds are characterized by BCP. The electron densities ρ(r), Laplacian of electron density $\nabla^2\rho(r)$, kinetic electron energy density G(r), potential electron energy density V(r) and total electron energy density H(r) at N- H···O and N- H···π BCP are collected in Table 7. The electron density value of all the complexes is in the range of hydrogen bonding. The strength of hydrogen bonding of all complexes is found in weak or medium range since it have positive $\nabla^2\rho(r)$ and positive H(r) values. The electron density at N- H···π BCPs in a2 and n2 stacking models are lesser than proposed criteria and are nearly 3 times lesser than N- H···O BCPs in **a1**, **n1** and **a3** complexes. This is due to large distance between hydrogen bonded atoms in stacking model, which are considered as very weak mixture of hydrogen bonding and van der Waals interaction. Aniline complexes have higher electron density at intermolecular hydrogen bond BCP than N-methylaniline complexes.

The existence of different types of non-covalent interactions can be established from NCI plots and plots of reduced density gradient (RDG) versus the electron density multiplied by the sign of the second Hessian eigenvalue (λ2)[36]. These plots are presented in Fig. 7. These plots indicate the presence of strong as well as weak interactions in the five models considered. Fig. 7 shows the low density, low-gradient spike lying at negative values in a1, a3 and n1complexes indicative of stabilizing interactions, probably through N– H···O hydrogen bond. It may be pointed out that in a3 complex there are two hydrogen bonds. The low density, low-gradient spikes lying at less negative values in a2 and n2 complexes indicate the presence of weak N- H···π interaction. The spikes lying at positive values are indicative of very weak van der Waals interaction. It may be noted that the λ2 as well as sign (λ2)ρ are more negative for a1 complex than those for n1 complex. This observation establishes our earlier conclusion that complex a1 is more stable the n1complex.

3.7. Interaction energy decomposition analysis

It is important to know the composition of total interaction energy

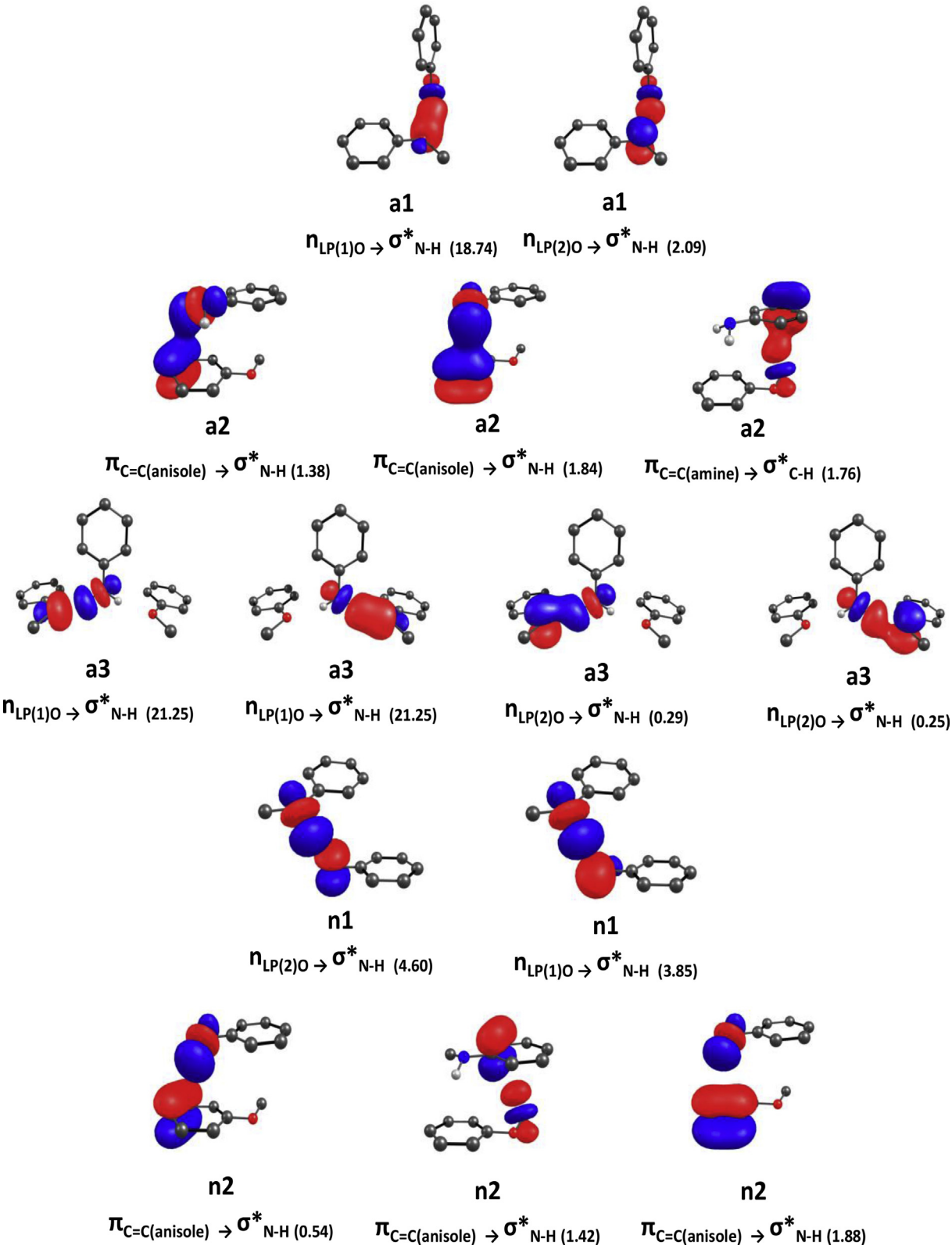

Fig. 5. NBO computed orbital interactions corresponding to a1, n1, a2 and n2of $\pi_{C=C(anisole)} \rightarrow \sigma^*_{N-H}$ and/or $\pi_{C=C(amine)} \rightarrow \sigma^*_{C-H}$. Second order interaction energies given in parentheses are present in kJ/mol.

and the effect of methylation on this composition. The total interaction energy obtained during complex formation can be decomposed into charge transfer, ionic and deformation terms [37]. Eq. (4) was used to calculate the total interaction energy. Counterpoise method of Boys and Bernardi were included to avoid basis set superposition errors (BSSE).

$$E_i = E_{ij}^{(2)} + E_Q + E_{DEF} + BSSE \quad (4)$$

Where E_i is the total interaction energy of complex with BSSE corrections, $E_{ij}^{(2)}$ is the charge transfer term, E_Q is the ionic energy and E_{DEF} is the monomer deformation energy. As it is known that total interaction

Table 6
The amount of charge transfer (in electrons), occupancies of interacting donor-acceptor natural bond orbitals (units are in a.u.), their second-order perturbation stabilization energies (kJ/mol)and deletion energy (kJ/mol).

Complex	Q_{CT}	Donor (Occupancy)	Acceptor (Occupancy)	ΔE^2	Deletion energy
a1	0.33	$n_{LP(1)O}$ (1.957) $n_{LP(2)O}$ (1.862)	σ^*_{N-H} (0.017)	18.74 2.09	57.07
n1	0.27	$n_{LP(1)O}$ (1.962) $n_{LP(2)O}$ (1.855)	σ^*_{N-H} (0.021)	3.85 4.60	24.87
a2	0.24 0.25	$\pi_{C=C(anisole)}$ (1.696, 1.711, 1.651)	σ^*_{N-H} (0.008) σ^*_{N-H} (0.008)	1.38 1.84	12.17
	0.16	$\pi_{C=C(amine)}$ (1.685, 1.705, 1.628)	σ^*_{C-H} (0.017)	1.76	
n2	0.24	$\pi_{C=C(anisole)}$ (1.695, 1.711, 1.651)	σ^*_{N-H} (0.018)	0.54 1.88	11.30
	0.18	$\pi_{C=C(amine)}$ (1.701, 1.717, 1.645)	σ^*_{C-H} (0.017)	1.42	
a3	0.36 0.36	$n_{LP(1)O}$ (1.956) $n_{LP(2)O}$ (1.862) $n_{LP(1)O}$ (1.956) $n_{LP(2)O}$ (1.862)	σ^*_{N-H} (0.018) σ^*_{N-H} (0.018)	21.25 0.29 21.25 0.25	117.38

energy in stacking complexes involve many other interactions along with N–H···π interaction, therefore only N–H···O type interactions are considered for further studies. The decomposition of energy data is given in Table 8.

The deformation energy of each monomer is obtained from the difference in energy between the optimized geometry of isolated monomer and the deformed geometry of monomer within the complex. E_{DEF} is calculated by adding deformation energy of all monomers involved in complex formation. The influence of E_{DEF} is small on total interaction energy. The charge transfer term $E_{ij}^{(2)}$ between interacting orbitals is obtained from NBO analysis. The ionic energy E_Q is calculated by substitution of all other terms in above equation. From energy decomposition analysis given in table, it is found that charge transfer is highest in **a3** and ionic interaction is highest in n1 complex.

4. Conclusion

The effect of methyl group substitution on the strength of H- bonding has been studied with aniline and N-methylanilines as H- donors and anisole as H- acceptor at ωB97X-D3/6–311++G (d,p) level of theory. We considered two types of interactions, namely, N- H···O and N- H···π in the formation of complexes. The possibility of both interactions was assured from molecular electrostatic potential map. The geometrical parameters and infrared spectra comparison showed red shift of N–H stretching frequency in all complexes. The π→π* transition in electronic spectra appeared between 220 and 240 nm and shifted to higher wavelength due to H- bonding. It may be noted that the charge transfer stabilizing energy

Table 7
Electron density ρ(r), Laplacian of the electron density $\nabla^2\rho(r)$, the kinetic energy density G(r), the potential energydensity V(r)and the total electron energy density H(r) (units are in a.u.) at BCPs of N- H···O and N- H···π type hydrogen bonds in both aniline and N-methylaniline complexes computed by QTAIM analysis.

complex	Atom Pairs	ρ(r)	$\nabla^2\rho(r)$	G(r)	V(r)	H(r)
a1	H29——O23	0.0184	0.0684	0.0149	-0.0127	0.0022
n1	H29——O23	0.0135	0.0436	0.0099	-0.0089	0.0010
a2	H29——C1	0.0064	0.0184	0.0040	-0.0034	0.0006
	H30——C4	0.0066	0.0184	0.0040	-0.0034	0.0006
	C13——H24	0.0064	0.0192	0.0041	-0.0034	0.0007
n2	H29——C3	0.0058	0.0180	0.0038	-0.0031	0.0007
	C17——H24	0.0057	0.0156	0.0034	-0.0029	0.0005
a3	H13——O26	0.0188	0.0712	0.0155	-0.0132	0.0023
	H14——O42	0.0188	0.0712	0.0155	-0.0132	0.0023

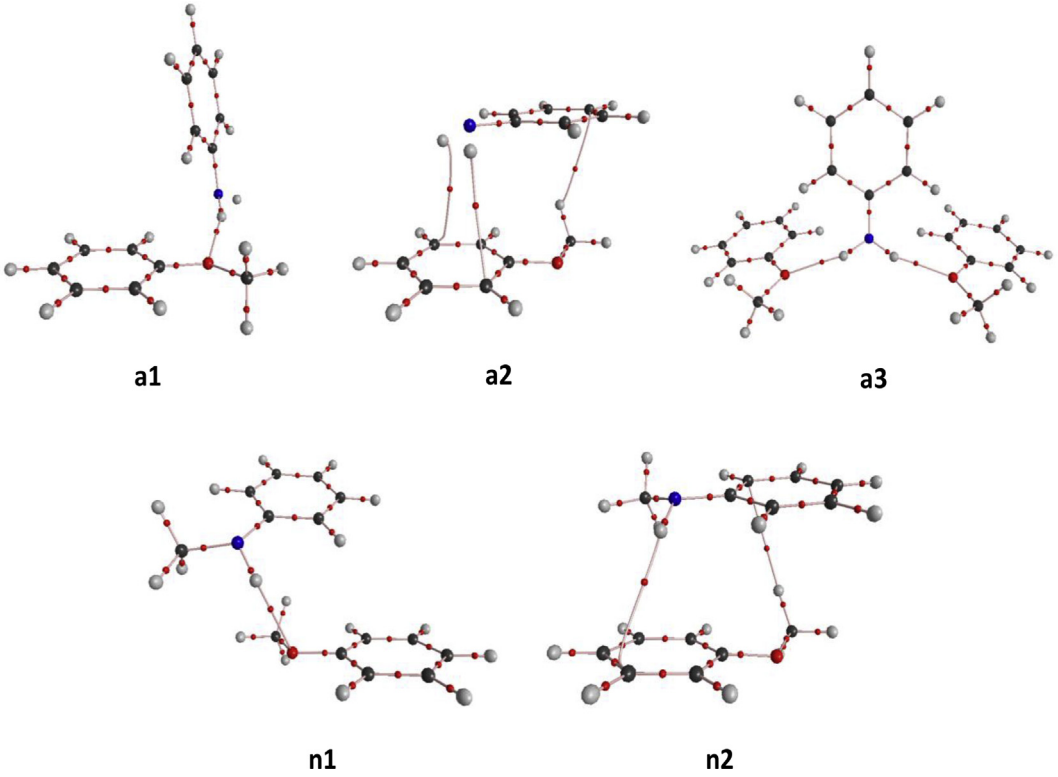

Fig. 6. Molecular graphs of a1, n1, a2, n2 and a3 complexes. Large circles correspond to attractors denote atomic positions: black-C, gray-H, blue-N and red-O. Small red circle denote bond critical points.

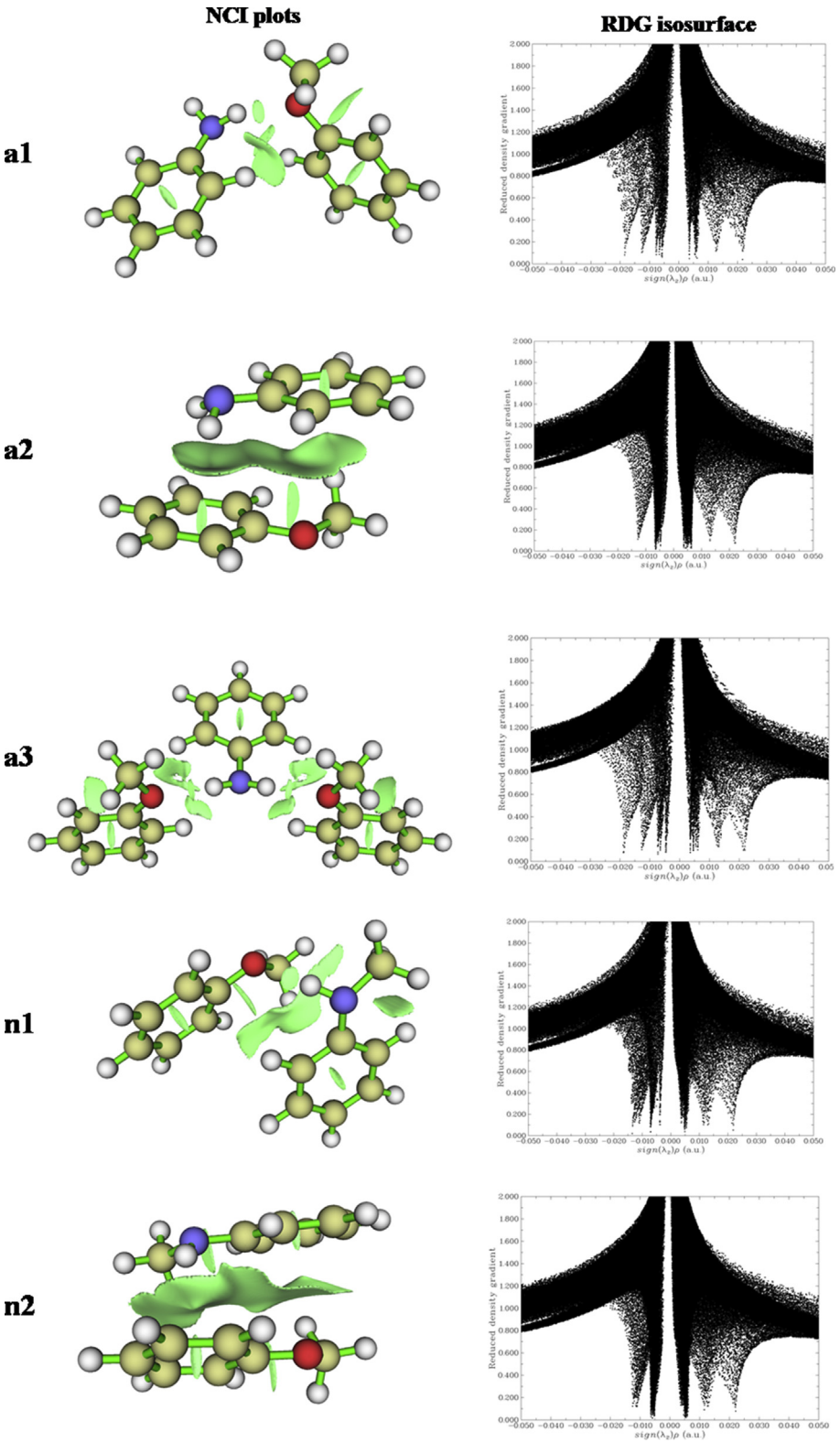

Fig. 7. NCI plots and plots of the RDG versus the electron density multiplied by the sign of the second Hessian eigenvalue (λ2) and RDG isosurface (s = 0.5) at the ωB97XD/6–311++G (d,p) level of the theory.

was higher for N- H···O interaction than N- H···π interaction. The hybrid orbitals of nitrogen atom are re-hybridized due to methyl substitution. This change in hybridization reduces C–N bond length due to increase in p-character and consequently N-methylaniline is made more planar than aniline. The AIM analysis at BCP on N- H···O and N- H···π interaction confirmed existence of H- bonding. The energy decomposition analysis provided evidence for increase in ionic energy with methyl substitution. The tuning of hydrogen bonding by changing substitution can find applications in biological systems, supramolecular chemistry and crystal engineering.

Table 8
Energy decomposition analysis (in kJ/mol) of a1, n1 and a3 complexes.

complex	E_i	$E_{ij}^{(2)}$	E_Q	E_{DEF}		BSSE
				aromatic amines	anisole	
a1	-25.00	-20.83	-8.01	0.18	0.43	3.23
n1	-30.76	-8.45	-27.05	0.85	0.34	3.55
a3	-48.52	-21.54-21.50	-12.09	0.49	0.32, 0.32	5.52

Declarations

Author contribution statement

Anil Singh Prohit: Conceived and designed the experiments.
R. Rajesh: Performed the experiments.
Madhavan Jacob: Analyzed and interpreted the data.
Justin Baskar, Raj Muhamed: Contributed reagents, materials, analysis tools or data.
Venu Kannappan: Conceived and designed the experiments; Wrote the paper.

Funding statement

This research did not receive any specific grant from funding agencies in the public, commercial, or not-for-profit sectors.

Competing interest statement

The authors declare no conflict of interest.

Additional information

No additional information is available for this paper.

References

[1] O.O. Brovarets, Y.P. Yurenko, D.M. Hovorun, Intermolecular CH···O/N H-bonds in the biologically important pairs of natural nucleobases: a thorough quantum-chemical study, J. Biomol. Struct. Dyn. 32 (2014) 993–1022.
[2] J. Šponer, J. Leszczynski, P. Hobza, Hydrogen bonding and stacking of DNA bases: a review of quantum-chemical ab initio studies, J. Biomol. Struct. Dyn. 14 (1996) 117–135.
[3] M. Brandl, M. Meyer, J. Sühnel, Quantum-chemical analysis of C-H···O and C-H···N interactions in RNA base pairs-H-bond versus anti-H bond pattern, J. Biomol. Struct. Dyn. 18 (2001) 545–555.
[4] S.K. Burley, G.A. Petsko, Amino-aromatic interactions in proteins, FEBS Lett. 203 (1986) 139–143.
[5] J.B.O. Mitchell, C.L. Nandi, I.K. McDonald, J.M. Thornton, Amino/aromatic interactions in proteins: is the evidence stacked against hydrogen bonding? J. Mol. Biol. 239 (1994) 315–331.
[6] J. Wang, L. Huang, R. Yang, Z. Zhang, J. Wu, Y. Gao, Q. Wang, D. O'Hare, Z. Zhong, Recent advances in solid sorbents for CO2 capture and new development trends, Energy Environ. Sci. 7 (2014) 3478–3518.
[7] G. Parthipan, T. Thenappan, Dielectric and thermodynamic behavior of binary mixture of anisole with morpholine and aniline at different temperatures, J. Mol. Liq. 138 (2008) 20–25.
[8] G. Piani, M. Pasquini, G. Pietraperzia, M. Becucci, A. Armentano, E. Castellucci, The anisole–ammonia complex: marks of the intermolecular interactions, Chem. Phys. Lett. 434 (2007) 25–30.
[9] R. Rajesh, R. Raj Muhamed, A. Justin AdaikalaBaskar, V. Kannappan, Ultrasonic and spectral studies on charge transfer complexes of anisole and certain aromatic amines, Chem. Phys. 478 (2016) 34–44.
[10] (a) K.C. Medhi, G.S. Kastha, Hydrogen bonding in aniline and some substituted anilines in different environments, Indian J. Phys. 37 (1963) 139;
(b) P.G. Puranik, K.V. Ramiah, Raman and infra-red spectra of amines, Proc. Indiana Acad. Sci. 54 (1961) 146;
(c) K.B. Whetsel, W.E. Roberson, M.W. Krell, Solvent and concentration effects on the near-infrared N–H bands of primary aromatic amines, Anal. Chem. 32 (1960) 1281;
(d) V.C. Farmer, R.H. Thomson, Inter- and intra-molecular hydrogen bonding in anilines, Spectrochim. Acta 16 (1960) 559–562;
(e) J.H.P. Utley, Solvent effects upon the first ultraviolet absorption band of substituted p-nitroanilines, J. Chem. Soc. 0 (1963) 3252–3260;
(f) A.B. Sannigrahi, A.K. Chandra, Hydrogen bonding effect on the electronic absorption of some secondary amines, J. Phys. Chem. 67 (1963) 1106–1109;
(g) J.L. Mateos, E. Diaz, R. Cetina, Desplazamiento quimico de la banda de protones unidos a nitrogeno, en los espectros de resonancia magnetica nuclear, Bol. Inst. Quim. Univ. Nacl. Auton. Mex. 14 (1962) 61;
(h) H. Suhr, Solvent effects on the nuclear magnetic resonance spectra of aromatic amines, Mol. Phys. 6 (1963) 153;
(i) C. Giessner-Prettre, M.J. Chauveau, Étude de l'influence de sels sur la largeur de la raie NH des spectres de résonance magnétique nucléaire de l'aniline et de la phényl hydrazine, Compt. rend. 254 (1962) 4450.
[11] (a) J.H. Lady, K.B. Whetsel, Infrared studies of amine complexes. I. Self-association of aniline in cyclohexane solution, J. Phys. Chem. 68 (1964) 1001–1009;
(b) W.B. Smith, The nature of the reaction of 2-methylpyridine with aniline and N-methylaniline, J. Org. Chem. 27 (1962) 4641–4643;
(c) J. Wimette, R.H. Linnell, Thermodynamics of H-bonding pyrrole-pyridines, J. Phys. Chem. 66 (1962) 546–548;
(d) H. Dunken, H. Fritzsche, Spektroskopische bestimmung der wasserstoffbrückenbindungsenergie in protonendonator-protonenakzeptor-Systemen IV. ergebnisse mit Indol als protonendonator, Z. Chem. 2 (1962) 379–380.
[12] (a) R.A. Nyquist, IR and NMR correlations for 3-x and 4-x substituted anilines, Appl. Spectrosc. 47 (1993) 411–422;
(b) K.B. Whetsel, J.H. Lady, Infrared studies of amine complexes. III. Association of aniline and N-methylaniline with benzene, N,N-dimethylaniline, pyridine, and N,N-dimethylcyclohexylamine, J. Phys. Chem. 69 (1965) 1596–1602;
(c) B. Ghosh, S. Basu, Studies on intermolecular π-hydrogen bond. Part 1, Trans. Faraday Soc. 61 (1965) 2097–2101;
(d) Z. Yoshida, E. Osawa, Intermolecular hydrogen bond involving a π-base as the proton acceptor. II. Interaction between phenol and various π-bases. Preliminary infrared study, J. Am. Chem. Soc. 87 (1965) 1467–1469;
(e) M. Oki, H. Iwamura, Steric effects on the O-H...π interaction in 2-hydroxybiphenyl, J. Am. Chem. Soc. 89 (1967) 567–579.
[13] S.R. Palit, S. Mukherjee, S.K.N.-H. De, Pi. Hydrogen bonding, J. Phys. Chem. 75 (1971) 2404–2405.
[14] M.J. Frisch, G.W. Trucks, H.B. Schlegel, G.E. Scuseria, M.A. Robb, J.R. Cheeseman, G. Scalmani, V. Barone, B. Mennucci, G.A. Petersson, H. Nakatsuji, M. Caricato, X. Li, H.P. Hratchian, A.F. Izmaylov, J. Bloino, G. Zheng, J.L. Sonnenberg, M. Hada, M. Ehara, K. Toyota, R. Fukuda, J. Hasegawa, M. Ishida, T. Nakajima, Y. Honda, O. Kitao, H. Nakai, T. Vreven, Montgomery Jr., J. A., J.E. Peralta, F. Ogliaro, M. Bearpark, J.J. Heyd, E. Brothers, K.N. Kudin, V.N. Staroverov, R. Kobayashi, J. Normand, K. Raghavachari, A. Rendell, J.C. Burant, S.S. Iyengar, J. Tomasi, M. Cossi, N. Rega, J.M. Millam, M. Klene, J.E. Knox, J.B. Cross, V. Bakken, C. Adamo, J. Jaramillo, R. Gomperts, R.E. Stratmann, O. Yazyev, A.J. Austin, R. Cammi, C. Pomelli, J.W. Ochterski, R.L. Martin, K. Morokuma, V.G. Zakrzewski, G.A. Voth, P. Salvador, J.J. Dannenberg, S. Dapprich, A.D. Daniels, Ö. Farkas, J.B. Foresman, J.V. Ortiz, J. Cioslowski, D.J. Fox, Gaussian 09, Revision B.01, Gaussian, Inc., Wallingford, CT, 2009.
[15] J.D. Chai, M. Head-Gordon, Long-range corrected hybrid density functionals with damped atom–atom dispersion corrections, Phys. Chem. Chem. Phys. 10 (2008) 6615–6620.
[16] S. Grimme, J. Antony, S. Ehrlich, H. Krieg, A consistent and accurate ab initio parametrization of density functional dispersion correction (DFT-D) for the 94 elements H-Pu, J. Chem. Phys. 132 (2010) 15104.
[17] R. Krishnan, J.S. Binkley, R. Seeger, J.A. Pople, Self-consistent molecular orbital methods. XX. A basis set for correlated wave functions, J. Chem. Phys. 72 (1980) 650–654.
[18] A.D. McLean, G.S. Chandler, Contracted Gaussian basis sets for molecular calculations. I. Second row atoms, Z=11–18, J. Chem. Phys. 72 (1980) 5639–5648.
[19] S.F. Boys, F. Bernardi, The calculation of small molecular interactions by the differences of separate total energies. Some procedures with reduced errors, Mol. Phys. 19 (1970) 553–557.
[20] V. Barone, M. Cossi, Quantum calculation of molecular energies and energy gradients in solution by a conductor solvent model, J. Phys. Chem. A 102 (1998) 1995–2001.
[21] M. Cossi, N. Rega, G. Scalmani, V. Barone, Energies, structures, and electronic properties of molecules in solution with the C-PCM solvation model, J. Comput. Chem. 24 (2003) 669–681.
[22] M.A. Thompson, ArgusLab 4.0.1, Planaria Software LLC, Seattle, WA, USA, 2004.
[23] E. Glendening, A. Reed, J. Carpenter, F. Weinhold, NBO, University of Wisconsin, Madison, WI, 1998.
[24] A.E. Reed, L.A. Curtiss, F. Weinhold, Intermolecular interactions from a natural bond orbital, donor-acceptor viewpoint, Chem. Rev. 88 (1988) 899–926.
[25] F. Biegler-König, J. Schönbohm, D. Bayles, AIM2000, J. Comput. Chem. 22 (2001) 545–559.
[26] Zhurko, G. A.; Zhurko, D. A. Chemcraft 1.6, http://www.chemcraftprog.com.
[27] C. Greve, E.T.J. Nibbering, H. Fidder, Hydrogen-bonding-induced enhancement of fermi resonances: a linear IR and nonlinear 2D-IR study of aniline-d_5, J. Phys. Chem. B 117 (2013) 15843–15855.
[28] L.K. Dyall, Solvent effects on the infrared spectra of anilines-V: anilines with no ortho substituents, Spectrochim. Acta A Mol. Spectrosc 25 (1969) 1423–1435.
[29] T. Nakanaga, K. Buchhold, F. Ito, Investigation of the NH-π hydrogen bond interaction in the aniline–alkene (C_2H_4,C_3H_6,C_4H_8) cluster cations by infrared depletion spectroscopy, Chem. Phys. 288 (2003) 69–76.
[30] K. Chandrasekaran, G3XMP2 inversion studies of heteroaromatic amines, N-aniline and N,N-aniline derivatives, Int. J. Pharm. Pharm. Sci. 7 (2015) 330–333.

[31] J.H. Lady, K.B. Whetsel, Infrared studies of amine complexes. IV. The N-H-O hydrogen bond in aromatic amine complexes of ethers ketones, esters, and amides, J. Phys. Chem. 71 (1967) 1421–1429.
[32] Q. Gu, C. Trindle, J.L. Knee, Communication: frequency shifts of an intramolecular hydrogen bond as a measure of intermolecular hydrogen bond strengths, J. Chem. Phys. 137 (2012), 091101.
[33] F. Weinhold, C.R. Landis, Discovering Chemistry with Natural Bond Orbitals, John Wiley & Sons, New Jersey, 2012.
[34] U. Koch, P.L.A. Popelier, Characterization of C-H-O hydrogen bonds on the basis of the charge density, J. Phys. Chem. 99 (1995) 9747–9754.
[35] P.L.A. Popelier, Atoms in Molecules: an Introduction, PrenticeHall, London, 2000.
[36] Erin R. Johnson, Shahar Keinan, Paula Mori-Sánchez, Julia Contreras-Garcıá, Aron J. Cohen, Weitao Yang, Revealing non-covalent interactions, J. Am. Chem. Soc. 132 (2010) 6498–6506.
[37] I. Rozas, I. Alkorta, J. Elguero, Hydrogen bonds and ionic interactions in guanidine/guanidinium complexes: a computational case study, Struct. Chem. 19 (2008) 923–933.